JETIR.ORG ISSN: 2349-5162 | ESTD Year : 2014 | Monthly Issue

JOURNAL OF EMERGING TECHNOLOGIES AND INNOVATIVE RESEARCH (JETIR)

An International Scholarly Open Access, Peer-reviewed, Refereed Journal

PROSPECTIVE MAPPING OF PYROPHYLLITE MINERAL DEPOSIT USING REMOTE SENSING IMAGERY OF PLATEAU STATE, NORTH CENTRAL NIGERIA

Danboyi Joseph Amusuk[1, 2], Chindo Musa Muhammad[1, 4], Mazlan Hashim[1], Amin Beiranvand Pour[3]

1. Geoscience and Digital Earth Centre (INSTeG), Research Institute for Sustainable Environment, Universiti Teknologi Malaysia, Johor Bahru, Skudai 81310, Malaysia
2. Waziri Umaru Federal Polytechnic, P.M.B. 1034, Birnin Kebbi, Kebbi State
3. Institute of Oceanography and Environment (INOS), University Malaysia Terengganu (UMT), Kuala Nerus 21030, Terengganu, Malaysia
4. The Federal Polytechnic Nassarawa, Nassarawa State, Nigeria

Abstract: Prospecting for Pyrophyllite mineralization by traditional means is a difficult and costly task because the deposits usually occur at schistose metamorphic rock environments, and hydrothermal veins that are rich with mica and quartz. However, this mineral has commercial and industrial importance so much so that the global market size for it was valued with **USD 151.7 million** in 2019 and is expected to keep growing at a compound annual growth rate (CAGR) of 5.7% from 2020 until 2027. The use of satellite multispectral remote sensing application to map the distribution is the best alternative as a fast and cost-effective way. The Landsat-8 (OLI) multispectral data was put forward in a greenfield prospective mapping to discriminate the potential areas of pyrophyllite mineral groups throughout Plateau state north central Nigeria. Band Ratios (BR) transformation and RGBs were the methods adopted for the detection at sub-pixel deposits of Al-rich, Fe^{3+}-rich, Fe^{2+}-rich and Mg-rich pyrophyllite. The outcome revealed the lithological units associated with pyrophyllite which are a clear differentiation of altered rocks, and the mineral sub-groups in them such as the Iron oxides, the ferric irons known to be in the metamorphic environments and the hydroxyl deposits known to be in regions of clay sedimentary rocks. Classification accuracies performed by confusion matrix revealed an overall accuracy at 92.3% with kappa of 0.9. This result show that the data has strong and sensitive bands that reacts positively with the complex terrain environments.

IndexTerms **- Pyrophyllite, Hydrothermal alteration, Landsat-8, Greenfield, Band Ratios.**

1. INTRODUCTION

The mineral Pyrophyllite is a form of talc with more of aluminium (Al) content instead of magnesium (Mg) $Al_2SiO_{10}(OH)_2$, which occur at regions that have undergone alterations (pour et al, 2020). They occur in varying color representation and usually around phyllite and schistose rock regions, where weathering processes had occurred (Nagy, 1995). The enrichment originates from (a). The changing phase of magnesium minerals such as serpentine, pyroxene, amphibole, olivine, in the presence of carbon dioxide and water. When this takes place, the process is called talc carbonation or steatization consequence of which we get a suite of talc. The reaction is serpentine + Carbon dioxide = talc +magnesium +water 2Mg3Si2O5(OH)4 + 3CO2 = Mg3Si4O10(OH)2 +3MgCO3 +3H2O. (b). It can also form by reaction of dolomite and silica, which is a typical type of skarnification of dolomite via silica-flooding in contact with metamorphic aureoles; dolomite + silica + water = talc + calcite + carbon dioxide; 3CaMg(CO3)2 + 4SiO2 +H2O = Mg3SiO10(OH)2 + 3CaCO3 + 3CO2. (c). Talc can also be formed from Magnesian chlorite and quartz in blue schist and eclogite metamorphism with the aid of the following reactions; chlorite + quartz= Kyanite + talc + water where the ratio of talc and Kyanite dependent on aluminium content with more aluminous rocks favoring the production of Kyanite (Pour et al, 2020). With remote sensing pyrophyllite can be detected through its capacity to distinguish the regions of associations of electronic transitions that reveal iron oxides (Fe) which are detected at the visible near infrared (VNIR), regions of Hydroxyl (OH) deposits, especially at the shortwave infrared

bands that range between (Pour and Hashim, 2013; Pour et al, 2018; Abubakar et al., 2019; Abubakar et al, 2019), and the associations with SiO4 vibrational radiations which in some sensors are detected at the thermal infrared (TIR) region (Rajendran and Nasir, 2019).

The nature of rock and topography of the Jos Plateau, it is difficult and costly to explore the mineralized area with traditional means but when the spectral, spatial and temporal resolutions of the data, is applied it is possible to differentiate between the regions of deposits yet, it is a commercial and industrial mineral with high demand and needed in a vast array of ways (Kauffman et al., 1974; Lohmander, 2000; Bhardwaj, 2001; Qin et al., 2020). Recent literature reveals that there has been a global shortage of supply of pyrophyllite in the market due to the industrial shutdown that has been triggered by the COVID 19 pandemic. This disruption and supply of the raw materials has hampered full-scale operations in several industries. Asia-Pacific region overtime has dominated the global use and demand for pyrophyllite on account of how there has been increasing investments that have been made with the product at several areas including construction activities and the automotive industry. The greatest concerns on this mineral is its contribution to Increasing urbanization and industrialization as development keeps growing around the world. A continental trend prediction is shown for 2015 – 2028, Figure 1.



Figure 1 Continental market trend of pyrophyllite between 2015 – 2028 from Cognitive Market Research, 2021.

The global pyrophyllite market size was valued in 2019 at **USD 151.7 million** and is expected to keep growing at a compound annual growth rate (CAGR) of 5.7% predicted from 2020 through 2027. More applied with increased demand in ceramics industry (MAR, 2020). Pyrophyllite has important properties of chemical inertness, high dielectric strength, high thermal conductivity, low electrical conductivity, and oil and grease adsorption, and has major applications are in ceramics, paint, paper, and plastics. Therefore, a clear knowledge of the rock of a region is very beneficial in so many ways. Figure 2 shows the market trend of the USA 2016-2027.

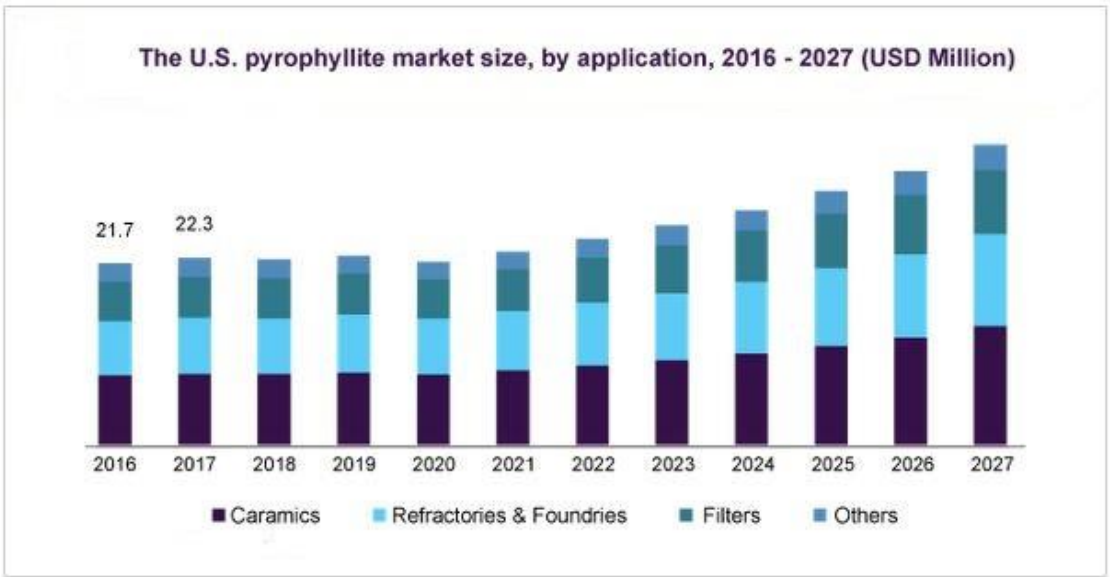

Figure 2 Pyrophyllite market growth by the US from 2016 – 2027(USD Million) from wwwgrandviewresearch.com

Plateau state north central Nigeria has been well known with tin exploitation since the early 70s, because of the nature of geology. There are eroded gneiss formations, granitic intrusions, and younger granitic rock

emplacements who are the host for tin (Sn) minerals. It is still believed that the region has potentials for the world's largest known deposits of columbite and the niobium ore which are all intertwined within each other. With long term processes of precipitation and weathering, several other categories of metallic deposits (Tantalite, wolfram, kaolin, zircon and uranium) have been traced to exist in the region and now the non-metallic pyrophyllite minerals are amongst the group of deposits that emanate from alteration activities around the kind of rocks existing on the Jos Plateau. With its versatility, and the kind of the geology of the environment, the mineral can boost the economy of Plateau state and Nigeria (Kauffman et al., 1974; Lohmander, 2000; Bhardwaj, 2001; Perkins, 2002; Qin et al., 2020).

This is hereby prospected in this study using remote sensing application covering the entire state as there is no recent regional geological remote sensing study for now that covers the entire state. This is with the bid to highlight the spread of this all important commodity in the state. Studies on the pyrophyllite reveal that a long time ago, they had been explored and mined globally by field and laboratory studies (Gruner, 1934; Wardle and Brindley, 1972; Lee and Guggenheim, 1981; Drits et al., 2012). In the recent times, satellite remote sensing has overtaken the regional mapping exploration exercises (Son et al., 2014; Qin et al., 2020; Portela et al., 2021). They are generally characterized to be found at regions of hydrothermal veins and as bedded deposits at regions of schistose rocks. And as it always is, that traditional regional mapping of these kind of deposit takes a lot of time and never cost effective. The fact remains that every mineral deposit most of the time indicate to have spatial relationship with hydrothermal alteration processes which overwhelms the immediate environment (Osinowo et al., 2021). This makes the content and distribution of the minerals in the surrounding to be in accordance with chemical interactions of the rocks and fluids in the environment that they go through (Pirajno, 1992).

The objective of this study was at providing a regional distribution map of high potential regions of the pyrophyllite mineral, using the Landsat-8 OLI in band ratio transformation spectral mapping procedure. And to evaluate the validation by the use of pseudo-accuracy assessment in confusion matrix.

2. Study area and Geological Setting

Plateau state is located geographically between latitude 08°24'N and longitude 008°32' and 010°38' east. Figure 3

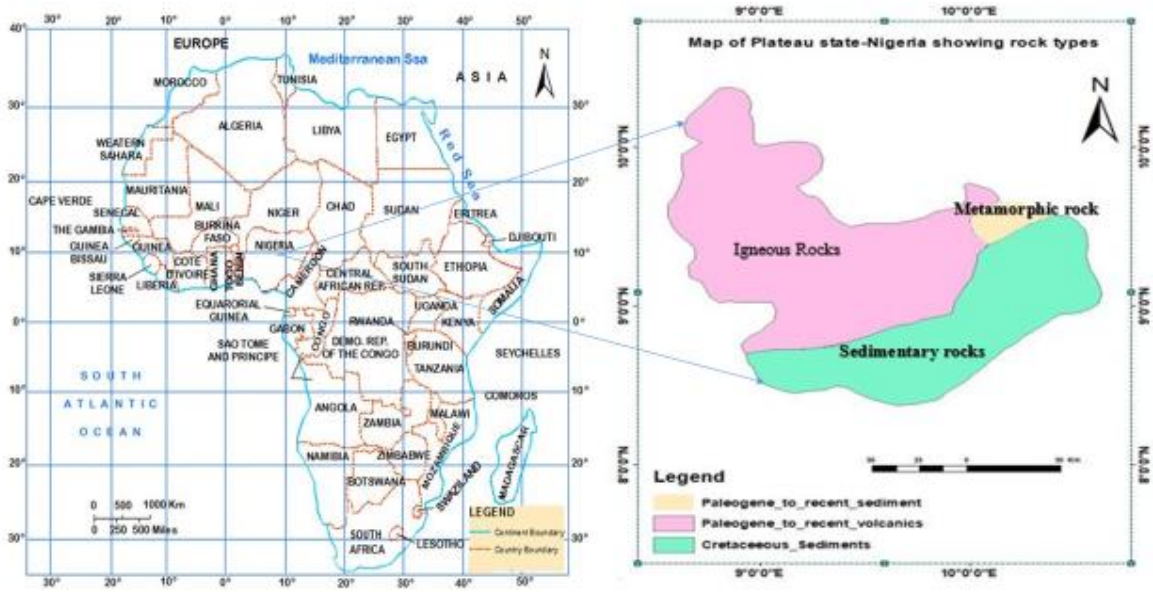

Figure 3 Plateau State North-Central Nigeria

The entire state is blessed with natural rock formations in form of hills and valleys and contains the three rock types. The land configuration has altitude differences with a range, the lower regions are about 200 - 300m and the high elevation between 1,200m - 1,829m above sea levels. The older granites are predicted back to the late Cambrian and Ordovician ages. The younger granites emplacements dates to the Jurassic period and can easily be differentiated by their ring formation doting the entire central Sahara. Also found within the landscape are many volcanic sheets of basaltic extruded rocks that are also classified to the Pliocene times. The younger granites have been the main sources of tin where their exploitation began at the beginning of the 19th century, during and after the colonial periods. Figure 1 shows an extracted geological map of Plateau from the geological map of Nigeria (Hodder, 1959).

3. Materials and Methods

In this study, the Landsat-8 OLI was applied to prospect for the potential regions of pyrophyllite distribution throughout the state boundaries. Table 1 summarizes the technical characteristics of the sensor data.

Table 1 characteristics features of Landsat-8 image data.

Band Number	Description	Wavelength µm	Resolution (m)
B1	Coastal / Aerosol	0.433 – 0.453	30
B2	Visible blue	0.450 – 0.515	30
B3	Visible green	0.525 – 0.600	30
B4	Visible red	0.630 – 0.680	30
B5	Near-Infrared	0.845 – 0.885	30
B6	Short wavelength infrared	1.56 – 1.66	30
B7	Short wavelength infrared	2.10 – 2.30	60
B8	Panchromatic	0.50 – 0.68	15
B9	Cirrus	1.36 – 1.39	30
B10	Long wavelength infrared	10.3 – 11.3	100
B11	Long wavelength infrared	11.5 – 12.5	100

The Landsat-8 data has been the continuity of land sat mission (LDCM) launched 11th February 2013 as a joint project of US Department of Interior of the Geological Surveys and the NASA (LDCM, 2013). Four scenes of cloud free and terrain corrected Landsat-8 Level L1T image data were freely downloaded from the U.S geological Surveys Earth Resources Observation and Science Centre (EROS) (http://earthexplorer.usgs.gov. The image data were downloaded for December 2019 the dry season period without rain and clouds, (path/Row 187-188/053-054). Figure 4 present a mosaic of the four scenes projected to UTM zone 32 N and in WGS-84 datum. The Landsat-8 sensor was formally called the Landsat data continuity Mission (LDCM), launched on February 11, 2013, from the Atlas-V rocket from the Vandenberg Air Force Centre, California and is still active beaming multispectral data of 550 scenes per day. This satellite image data remains a staple and an open source data for the public free use.

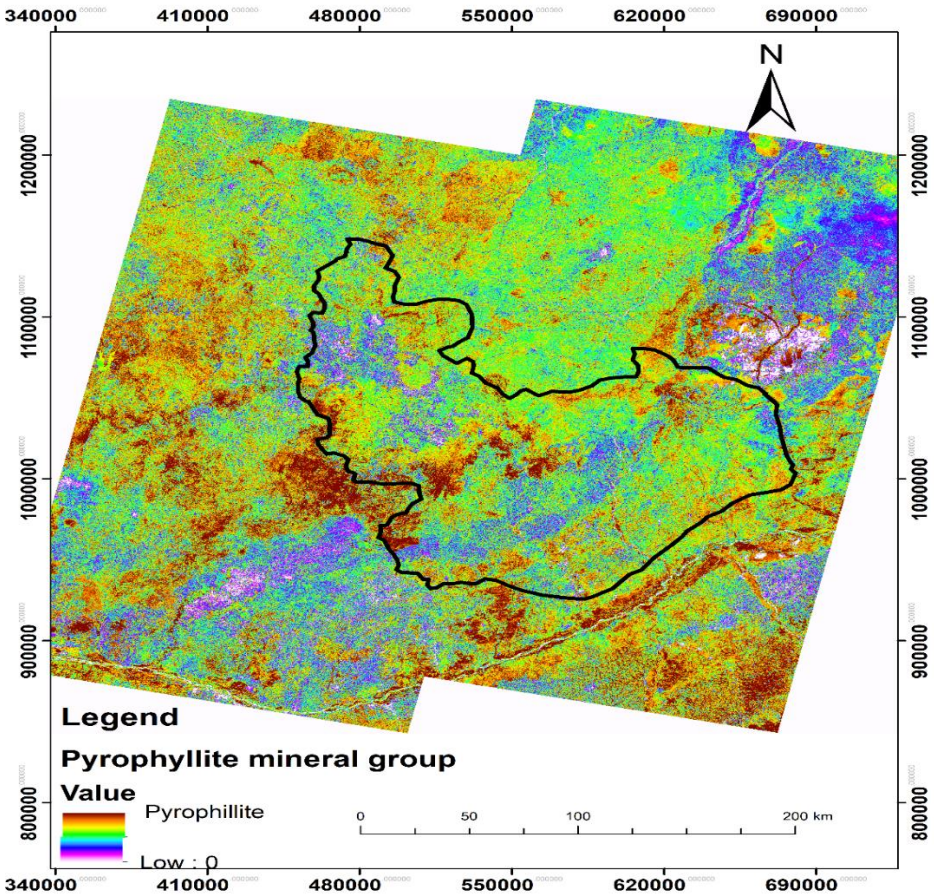

Figure 4 Mosaic of 4 scenes and boundary line of Plateau state

3.1. Pre-processing of Landsat-8 Datasets

Four (4) scenes of data were stacked mosaicked and Pre-processing through conversion from the original GeoTIFF format to the standard Envi format, conversion to radiance using Envi 5.3 software, and atmospherically corrected using the Fast Line-of-sight Atmospheric Analysis of Spectral Hypercubes (FLAASH) model. The band ratio transformation technique is highly respected in geological mapping because of the capacity to divide data bands and produce results that are accurate while caring for effects of topography, shadows, aspects and solar viewing angles of the sensor and their effects to the data. This follows vast use in geological application (Pour et al., 2020).

The USGS spectra for Pyrophyllite was extracted and superimposed on the spectral bands of Landsat-8/OLI, with an indication of the convolve of B2, B4, B5, B6 & B7, the selected bands for RGB and BRs Figure 5.

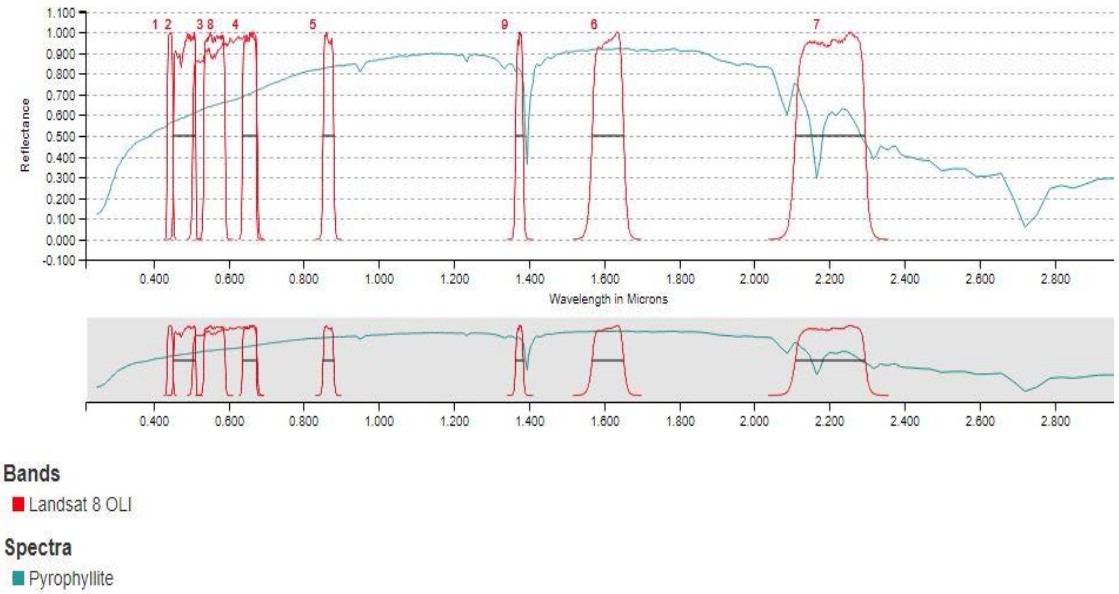

Figure 5 Spectral Curve of Pyrophyllite on Landsat-8 bands

The spectral curve indicates the hotspot areas of High reflectance from (0.400 - 1.390) and a sharp absorption at 1.400, and high reflectance again to (2.000) the absorption at (2.100-2.360) from absorption for pyrophyllite minerals which fall under the clay absorption region at B6 (1.400**µm)** and B7(2.1-2.36) wavelength range. Also with some small indications at (0.95µm, 1.25µm). Based on the display of the spectral curve of the mineral type the bands were selected. Channel combination of red, green and blue color panels (RGB) of B7, B6 & B2 represents SWIR-2 (7), SWIR-1 (6), and blue (2). This band combination is particularly useful for identifying geological formations, lithology features, and faults (Araujo et al, 2013). The identification of iron oxides is best located at B2 and B4 of the Landsat-8 (OLI) and band ratios generated to highlight the alteration areas of the associated minerals to pyrophyllite. Several literatures on applications of BR techniques in mapping both lithology and mineral resources exist, and each explains how successful they reveal mineral alteration areas (Pour and Hashim, 2020). With Landsat 8, the charge transfer absorption of iron oxides is best detected at B4/B2, as vividly explained by (Ducart et al, 2016). Figure 6 presents how robust the ratio performs, with regions of iron in the black and white image depicted in white patches.

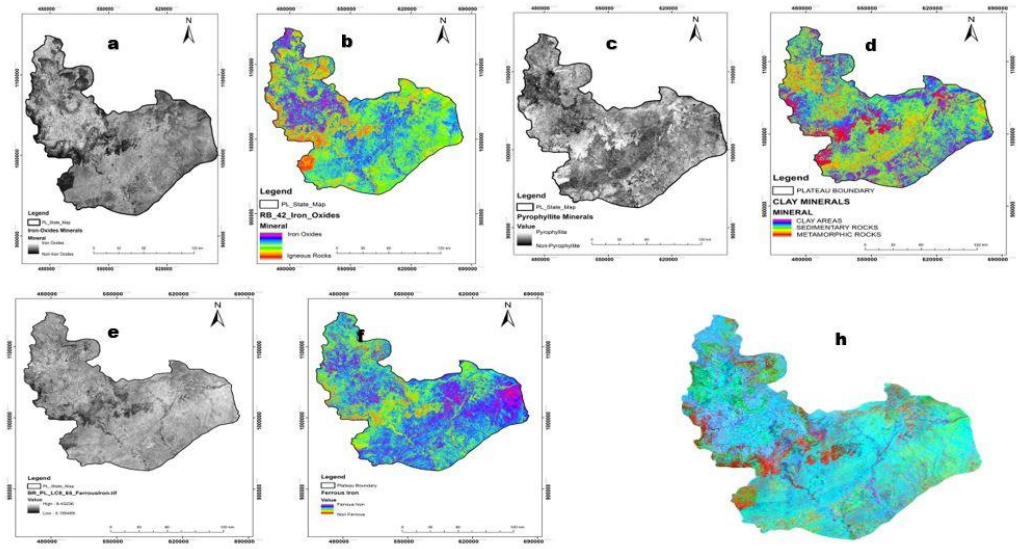

Figure 6 Results of pyrophyllite group (a), (b) gray scale of Iron oxides BR 4/2, (c), (d) gray scale images of Clay BR 6/7, (e), (f) Gray scale images for Ferrous irons BR6/5. (h) RGB of the 3 rations.

The mapping of clays with Landsat-8 (OLI), produces high reflectance more prominent at B6, B7, but based on the spectral reflectance's of this bands, band ratio transformation was applied because of the nature of the terrain. But at these bands, a strong absorption of features is experienced near 2.2 - 2.3 µm which is at B7, and the common deposits found to exist at this region includes hydroxyl-bearing minerals (clay and mica minerals), hydrated sulfates (gypsum and alunite), and, reluctantly carbonate minerals (calcite and dolomite), (Rowan et al. 1974, Goetz & Rowan 1981; **Knepper 1989;** Pour and Hashim, 2015). while BR 6/5 discriminate ferrous minerals respectively., highest reflectance difference between Landsat-8/OLI bands 6 and 5, with a high absorption in band 5 as a result of high iron oxide abundance. and RGB 4/2, 6/7, 6/5 have been applied for both lithological and alteration mapping. The results usually show iron-oxide region in red, Clay and hydroxyl rich areas appear yellow and ferrous minerals show up in blue colour in the RGB (Figure 6h).

4. Results and discussion

The reflectance spectra of iron oxides and vegetation are very comparable in the wavelength ranges that bands 1 and 2 of the Landsat-8/OLI satellite cover, with band 3 deviating only very slightly from this pattern. The maximum amount of reflectance of vegetation is identified at band 3, and the numerical value for vegetation is relatively similar with that of goethite rocks. On the other hand, the reflectance of hematite at the same band 3 will be noticed to be lower than that of goethite and vegetation. As a consequence of this, the first three bands are not particularly not too good to be applied for discriminating between different types of iron oxides in areas that are heavily covered by vegetation. At band 4 clay minerals, iron oxides (including hematite and goethite) have a high reflectance, while chlorophyll of green plants reveal a very significant absorptive capacity to light at the red wavelengths (band 4). Iron oxides exhibit high absorption behaviour at the region of band 5. Therefore, bands 4 & 5 of the Landsat-8/OLI image can highly beneficial when applied to differentiate between the distribution of flora and places that contain iron oxides. Therefore, the spectral bands 1 – 6 of the Landsat-8/OLI are good to be applied for rocks, vegetation and mineral resources that are in the class of clays respectively. Despite that the reflectance of clay minerals is higher than that of iron oxide and of vegetation. While clay minerals exhibit an absorption feature in the region of the electromagnetic spectrum that is covered with Iron oxides do not exhibit any diagnostic spectral characteristics in the SWIR range when viewed with Landsat-8/OLI band 7's spectral resolution. It is usual to practice using band 6 and 7 are used for the detection of clay minerals (Rowan et al. 1974, Goetz & Rowan 1981). Clay minerals have high absorption in band 5 due to the presence of a significant amount of iron oxide. Spectral band ratios employed in the Landsat-8/OLI imagery revealed significant absorption at regions of bands that are relatively close together.

5. Conclusion

This study investigated the capability of the Landsat-8 OLI in revealing the regions of pyrophyllite distribution covering Plateau state. The performance of the band ratio transformation was evaluated covering the VNIR and the SWIR portions of the data. The delineated zones of hydrothermal alteration zones are revealed more at the leeward sides of the mountainous regions. There is very strong structural influence from the upper Plateau that constitute more of the regions of igneous rocks. Landsat-8/OLI remote-sensing data,

for detection of igneous rock is very effective. Iron oxides and clay minerals associated to iron deposits have been detected using this approach. Specifically, band ratio (4+6)/5 showed the best results for mapping high-grade iron ore areas. Band ratio 4/2 correctly highlights iron oxides mainly related to mafic The result of the Landsat-8/OLI band ratio 6/7 divided by the ratio 5/4 produced an adequate index for detection of clay minerals.

References

1. Abubakar, A. J. A., Hashim, M., & Pour, A. B. (2019). Identification of hydrothermal alteration minerals associated with geothermal system using ASTER and Hyperion satellite data: a case study from Yankari Park, NE Nigeria. *Geocarto International*, *34*(6), 597-625.
2. Abubakar, A. J. A., Hashim, M., & Pour, A. B. (2019). Remote sensing satellite imagery for prospecting geothermal systems in an aseismic geologic setting: Yankari Park, Nigeria. *International Journal of Applied Earth Observation and Geoinformation*, *80*, 157-172
3. Bhardwaj, R.K., (2001). Modelling the barrier properties of polymer-layered silicate nanocomposites, macromolecules, 34: pp, 9189-9192.
4. Ducart, D.F. Silva, A.M. Toledo, C.L.B. De Assis, L.M. Mapping iron oxides with Landsat-8/OLI and EO-1/Hyperion imagery from the Sierra Norte iron deposits in the Carajás Mineral Province, Brazil Brazilian J. Geol., 46 (3) (2016), pp. 331-349
5. Drits, V.A., Guggenheim, S., Zviagina, B.B., Kogure, T. (2012) Structures of the 2:1 layers of pyrophyllite and talc. Clays and Clay Minerals: 60: 574-587.
6. Goetz A.F.H., Rowan L.C. 1981. Geologic remote sensing. Science, 211:781-791.
7. Gruner J W (1934) *The crystal structures of talc and pyrophyllite* Zeitschrift fur Kristallographie 88 412-419
8. Hodder, B. W. (1959). "Tin Mining on the Jos Plateau of Nigeria". Economic Geography. **35** (2): 109–122. doi:10.2307/142394. ISSN 0013-0095. JSTOR 142394.
9. Kauffman, S. H., Leidner, J., Woodhams, R. T., & Xanthos, M. (1974). The preparation and classification of high aspect ratio mica flakes for use in polymer reinforcement. *Powder Technology*, *9*(2-3), 125-133.
10. Knepper Jr. D.H. 1989. Mapping hydrothermal alteration with Landsat Thematic Mapper data. : Lee K. (ed.). Remote sensing in exploration geology - A combined short course and fieldtrip. 28º International Geological Congress Guidebook T182, p. 13-21.
11. LDCM Landsat Data Continuity Mission 29th Annual Louisiana RS/GIS Workshop April 23, Cajundome Convention Center, Lafayette, Lousiana, 2013.Landsat
12. Lee J H, Guggenheim S (1981) *Single crystal X-ray refinement of pyrophyllite-1Tc* American Mineralogist 66 350-357
13. Lohmander, S. (2000). Influence of shape and shape factor pigment particles on the packing ability in coating layers. Nordic pulp and paper Research Journal, 15(3), pp 300-305.
14. Market Analysis Report, 2020. Pyrophyllite Market Size, Share & Trends Analysis Report By Application (Refractories & Foundry, Ceramics, Fillers), By Region (APAC, North America, Europe, Central & South America, MEA), And Segment Forecasts, 2020 – 2027. Report ID: GVR-4-68038-834-3
15. Ninomiya, Y.; Fu, B. Thermal infrared multispectral remote sensing of lithology and mineralogy based on spectral properties of materials. *Ore Geol. Rev.* **2019**, *108*, 54–72.
16. Perkins, D. 2002. Mineralogy. 2nd ed. New Jersey: Prentice Hall.315.
17. Pirajno F. Hydrothermal Mineral Deposits, Principles and Fundamental Concepts for the Exploration Geologists Springer, Berlin (1992)
18. Pour, A. B., & Hashim, M. (2013). Fusing ASTER, ALI and Hyperion data for enhanced mineral mapping. *International Journal of Image and Data Fusion*, *4*(2), 126-145.
19. Pour, A.B.; Park, Y.; Park, T.S.; Hong, J.K.; Hashim, M.; Woo, J.; Ayoobi, I. Regional geology mapping using satellite-based remote sensing approach in Northern Victoria Land, Antarctica. *Polar Sci.* **2018**, *16*, 23–46.
20. Pour A.B., Sekandari, M., Rahmani, O., Crispini, L., Laufer, A., Park, Y., Hong, J.K., Pradan, B., Hashim, M., Hossain, S., Muslim, A., Mehranzamir, K. 2020. Identification of Phyllosilicates in the Antarctic Environment Using ASTER Satellite Data: Case Study from the Mesa Range, Campbell and Priestley Glaciers, Northern Victoria Land. Remote Sensing, vol 13 (1), 38 https://doi.org/10.3390/rs13010038
21. Pour, A. M. Hashim Hydrothermal alteration mapping from Landsat-8 data, Sar Chesmeh copper mining district, south-eastern Islamic Republic of Iran J. Taibah Univ. Sci., 9 (2015), pp. 155-166
22. Rajendran, S.; Nasir, S. ASTER capability in mapping of mineral resources of arid region: A review on mapping of mineral resources of the Sultanate of Oman. *Ore Geol. Rev.* **2019**, *108*, 33–53.

23. Robinson, G., Van Gosen, B., and Foley, N. (2006) Ultra-mafic hosted talc deposits. USGS
24. Rowan L., Wetlaufer P., Goetz A., Billingsley F., Stewart J. 1974. Discrimination of rock types and detection of hydrothermally altered areas in south-central Nevada by the use of computer-enhanced ERTS images. U.S. Geological Survey Professional Paper, 883, 35 p
25. Son, Y., Kang, M and Yoon, W. (2014). Pyrophyllite mapping in the Nohwa deposit, Korea, using ASTER remote sensing data. Geosciences journal, vol 18, No 3, p, 295 – 305.
26. Thiago P. de Araujo, Fernando Machado de Mello, Essaïd Bilal. Comparison between IHS-RGB transformations and ratio bands methods from LANDSAT imagery in the Rio de Janeiro region, Brazil. Carpathian Journal of Earth and Environmental Sciences, North University Center of Baia Mare, Romania, 2013, 8 (1), pp.99-104. ffhal-00783144
27. Yariv, S. 1992. Wettability of clay minerals, in modern approaches to wettability, M.E. Schrader and I.L George, Editors, Plenum press: New York. P.179-326.
28. Wardle R, Brindley G W (1972). The crystal structures of pyrophyllite, ITC, and of its dehydroxylate. American Mineralogist 57 732-750.